Acid Mine Drainage in the Chinkuashih-Shuinantung Area

LOUIS L. TSAI *, CHOW-SON CHEN*, AND LI-CHUNG SUN*

(Received 30 June 1991; Revised 4 December 1991)

ABSTRACT

The Chinkuashih-Shuinantung area is mainly composed of outcrops from the Miocene Nankang Formation. Crustal movements after the late Pliocene have led to several high-angle faults and lifted the Shitih Formation to the surface. During the Pleistocene, dacite intruded into Miocene sediments and thereafter hydrothermal gold-copper ore deposits were formed. These deposits are composed mostly of metal sulfides ,including pyrite, enargite, galena, tetrahedrite, and sphalerite, together with limited native gold. All these sulfides may produce acid mine drainages. The river bed course of the Chiufen Chi is rather close to the fault traces, indicating a close relationship between water flow systems and tectonic movements.

Water and soil samples were collected from several selected sites, including the upper, middle, and lower stream areas of the Chiufen Chi; along with the west, south, and east banks of the Shuinantung Bay; in addition, mine waters drained directly from the Penshan 5th adit and 7th adit were also collected near their portals. Geochemical data such as pH value, water temperature, turbidity, conductivity, dissolved oxygen, and selected ionic concentrations, were measured later. All samples were collected and analyzed during each season of a year. The results indicate that water drained from the two mine adits and the lower stream area of the Chiufen Chi exhibit low pH values, high metal (esp. Cu and Fe) and sulfate contents, and great conductivities. The acid mine drainage effect is very obvious, especially during the rainy season.

The Transient Electro-Magnetic (TEM) method,using square loops 20 *m* on a side, was also applied in this area for prospecting purposes. Measured transient voltages were inverted in terms of 1-D models. Four-layered models consisting of low-high-low-low resistivity patterns best fit the 49 coincident loop data. The effective exploration depth was between 5 *m* to 50 *m*. Furthermore, resistivities measured along the Chiufen Chi varied with the season, indicating high porosity and permeability in rocks underlying the study area, probably due to ore mineralization , faults or joints;on the other hand, resistivities measured along the Shuinantung Bay are not affected by seasonal change, indicating a saturated aquifer underneath the area near the sea.

* *Institute of Geophysics, National Central University*

1. INTRODUCTION

"Shuinantung" is a concave-shaped bay on the northern coast of Taiwan. Yellowish colored pollutants in this area had been noted for several decades. They contrasted sharply with the blue sea water nearby and was nick-named the Yinyan Sea by local residents. Effluents from the Taiwan Metal Mining Corp. plant, located near the south bank of Shuinantung Bay, were blamed for this pollution, even though the plant itself has been shut down since 1987. The southern inland area of Shuinantung is the Chinkuashih gold-copper ore district. This area had been mined since early this century. Wang (1953, 1955, 1973), Huang (1955, 1963), Juan *et al.* (1959), Tan and Yu (1968), Yen (1974), Huang and Yeh (1977), and Chen (1986) provide detailed geologic background informations about this area.

The purpose of this study is to investigate the geologic factors which are responsible for the marine pollution in the Chinkuashih-Shuinantung area. The methods of investigation are as follows: (1) Geological survey and structural investigation; (2) Geochemical soil and water (including stream and mine effluents) samples were collected and analyzed so as to detect their pH values, conductivities, turbidities, dissolved oxygen, and selected ionic concentrations; (3) The Transient Electro-Magnetic (TEM) method was performed in the area in order to evaluate flow patterns of ground water, and stratigraphic structures. The geochemical analyses and geophysical prospecting were executed in late August and October of 1989 in addition to mid-January and early in May of 1990 respectively, so as to evaluate the seasonal changes of surface water, ground water, and soil characteristics.

2. GEOLOGICAL INVESTIGATION

The maximum altitude of the study area is over 700 meters above sea level, in the southeastern part of this area. Figure 1 shows evenly distributed topographic contours with rather steep slopes. The Chiufen Chi is the main river in the area. Its river course and flow pattern are rather close to the known fault traces, indicating the influences of fracture zones. The outcropped strata include the Miocene Juifang Group with the Nankang Formation and the underlying Shitih Formation. Crustal movements after the late Pliocene led to several high-angle faults (mostly normal faults striking N-S and E-W) that lifted the Shitih Formation to the surface. During Pleistocene times, dacite intruded into the Miocene sediments, and thereafter hydrothermal gold-copper ore deposits were formed (see Figure 2). The outcropped stratigraphic units are described as follows:

(1) The Shitih Formation: sparsely distributed in the Chinkuashih mine and village areas, consists of gray colored, fine- to medium- grained sandstones

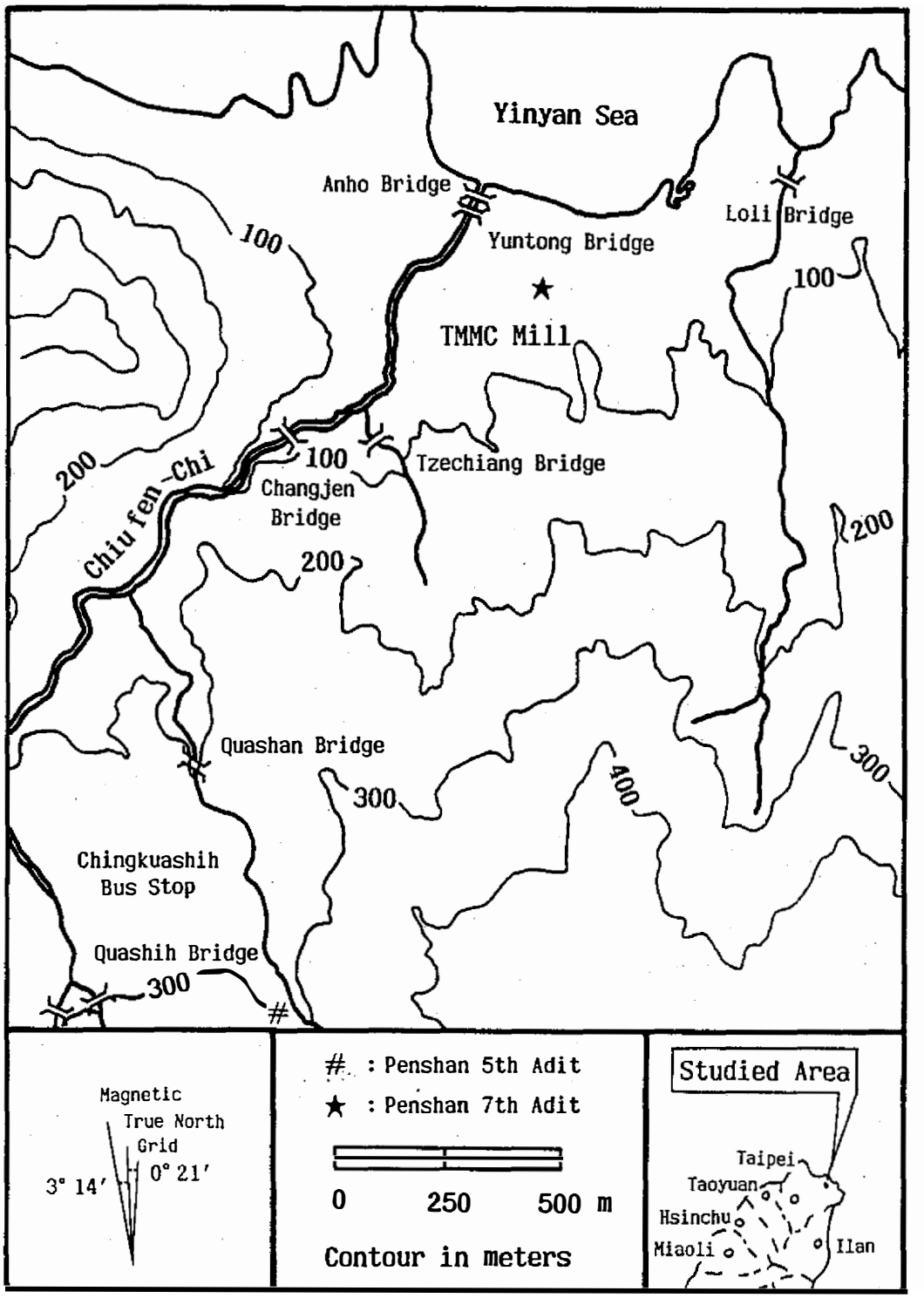

Fig. 1 Contour map of the study area (TMMC: Taiwan Metal Mining Corporation).

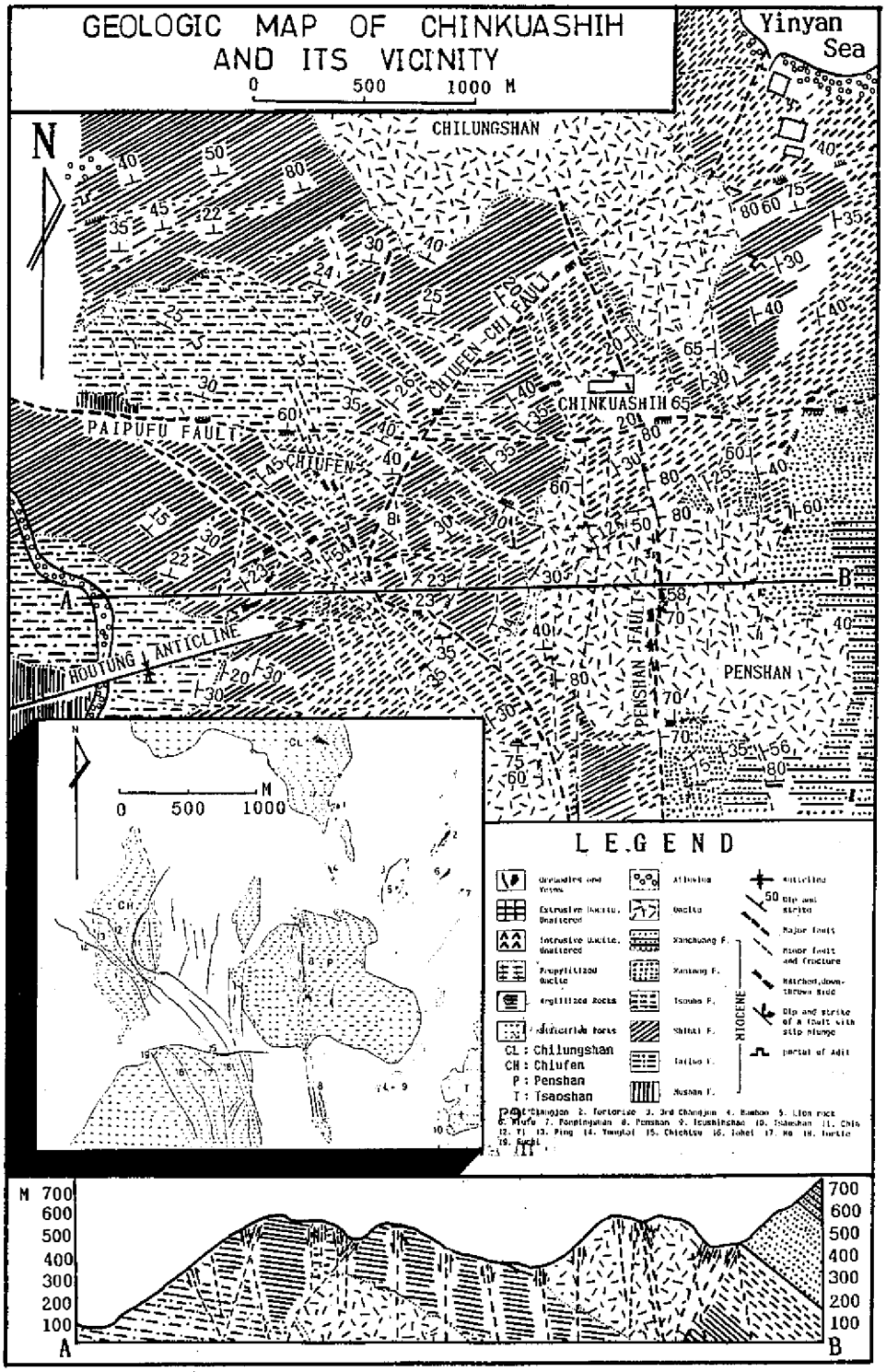

Fig. 2 Geological map and ore bodies in the Chinkuashih area (after Wang, 1973).

interbedded with gray to dark shales, thin coal seams and coaly shales.

(2) The Nankang Formation: includes Nankang Sandstone and the underlying Tzoho Formation. This formation is the most common sedimentary stratigraphic unit in this area, distributed along routes near the sea and between Chinkuashih and Shuinantung in addition to the southeastern part of this area. The Nankang Sandstones are bluish-gray colored, calcareous, thick, and of shallow-water origin. Whereas the Tzoho Formation consists of dark gray shale on top of yellowish-gray, fine-grained graywacke and is also of shallow-water origin.

(3) Dacite: including Chilungshan, Chiufen, and Chinkuashih bodies, outcropped mostly along the Chiufen Chi. Their lithologic compositions are biotite-pyroxene dacite, biotite-hornblende dacite, bio-horn-pyro dacites, and hornblende dacite. The grayish-white color turns dark green after weathering or hydrothermal alterations. The dacites are commmonly associated with gold and copper mineralization.

The most important ore deposits in the study area are the Penshan and the Changjen ore bodies located in the southern part of this area. These deposits are composed mostly of metal sulfides, including pyrite,enargite, galena, tetrahedrite, and sphalerite, together with native gold. The sulfides are responsible for the production of acid mine drainages.

3. GEOCHEMICAL ANALYSES

Sample sites are shown in Figure 3. Water samples were collected from mine effluents near the portals of the Penshan 5th and 7th adits; the upper, middle, and lower stream sections of the Chiufen Chi; and from a small gully over the eastern Shuinantung Bay. Soil samples were also collected along the Chiufen Chi and along the Shuinantung Bay. Eleven water samples and eight soil samples were collected during esch season of a year. Water temperature, turbidity, dissolved oxygen, conductivity, and pH value were measured with a water quality detector while sampling. Total sediment (TS) and suspended sediment (SS) were determined by filtering and weighing. Chemical oxygen demand (COD) was detected using a IIJIMA C303 COD Meter. Sulfide and NH_3 contents were determined by CNS-K9070 and CNS-K9099 Spectrum Absorptions respectively. Sulfate content was detected using the $BaCl_2$ precipitation method. Total hardness (Ca and Mg) was decided by EDTA titration. Finally, metal contents including Fe, Cu, Zn, Mn, Pb were measured by Atomic Absorption. Soil samples were prepared by both water-wash and nitric acid-wash before analyzing.

The results of geochemical analyses are listed in the appendix, and are summarized as follows:

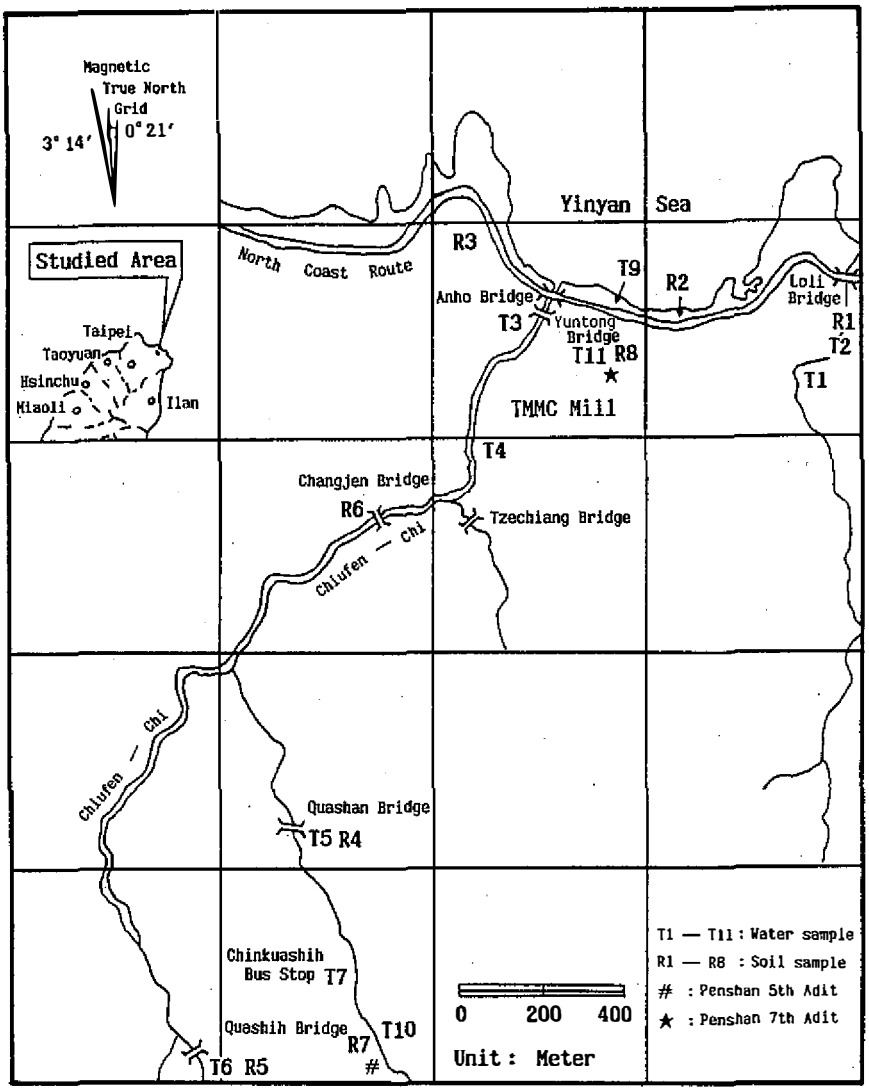

Fig. 3 Water and soil sample locations.

(1) Mine effluents from the Penshan 5th and 7th adits exhibit strong acidity and great conductivity; high total sediment, metal(esp Cu and Fe), and sulfate contents. Furthermore, the phenomena are not affected by seasonal changes, implying an acid mine drainage effect(see Figure 4).

(2) The effluents from the Penshan 5th adit and the Chiufen Chi are two main sources of the pollutants in the Shuinantung Bay. Both of them can be directly or in directly related to acid mine drainages in the study area.

(3) Metal content as analyzed from water-washed soil samples may not include all of the metal attached. On the other hand, metal content as analyzed from nitric acid-washed samples may include primary metals to a certain

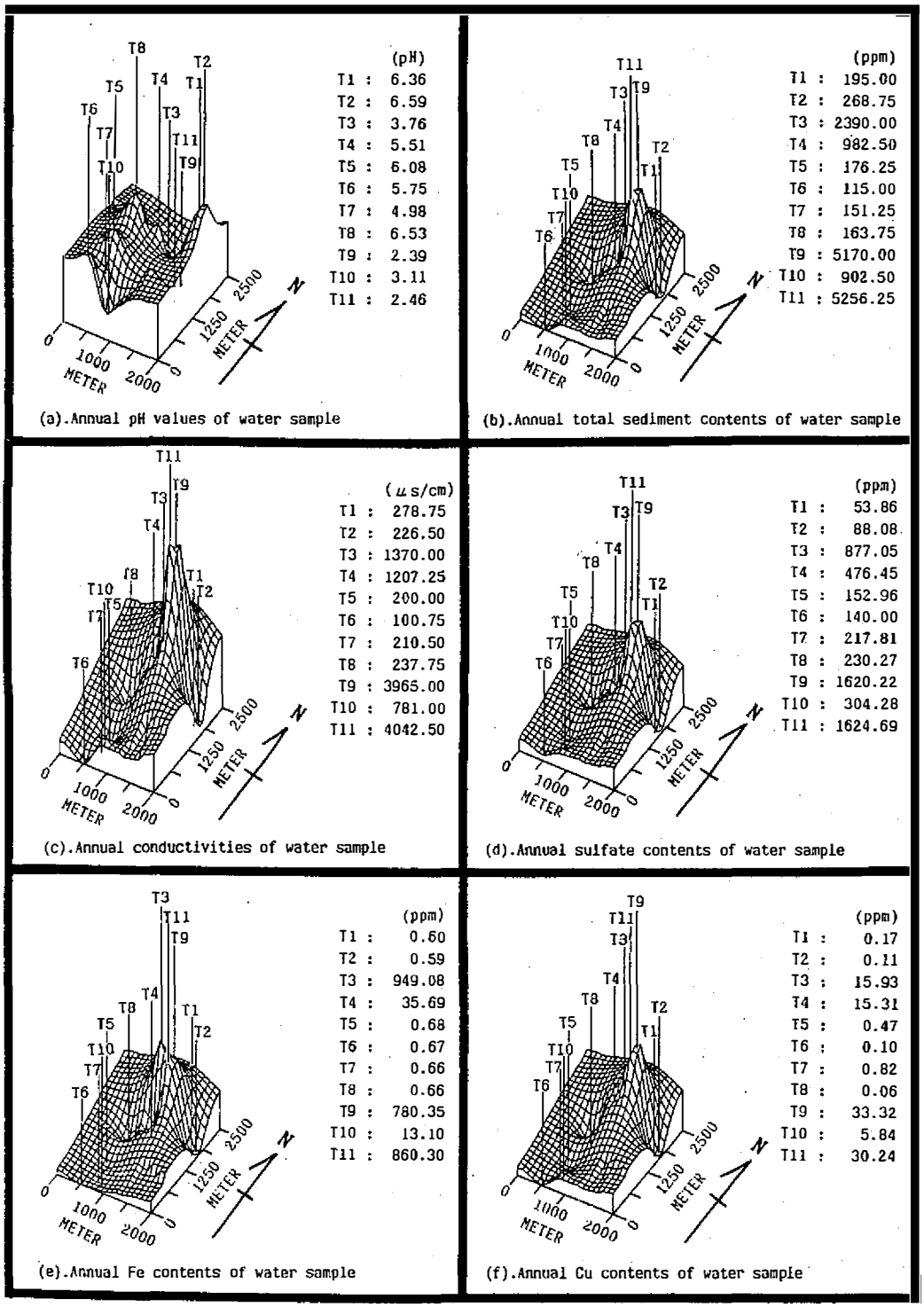

Fig. 4 (a)~(f). 3-D plots of some geochemical parameters in the study area, T1~T11 Sample sites as shown in Figure 3.

extent. Therefore, results of soil sample analysis can only be compared between sample sites, on a qualitative basis.

(4) Soil samples collected near the portal of the Penshan 7th adit also show strong acidity and high metal content during each season of a year. However, this is not so for soils collected near the portal of the Penshan 5th adit; Obviously the acid mine drainage reaction is more complete in the lower 7th adit than in the higher 5th adit.

(5) Mine effluents contain less dissolved oxygen compared to the surface waters, indicating an anerobic and reductive environment in the underground workings.

(6) The chief metal pollutants in the study area are iron and copper, with zinc, manganese, and lead next; the main nonmetal pollutants in this area are sulfide sulfur and sulfates.

(7) The chemical composition of the stream water in the Chiufen Chi more or less reflects seasonal and precipitational changes. On the other hand, those from the mine drainages were nearly stable throughout the whole year. However, the change of chemical compositions in the acid mine drainage is more obvious during the rainy season, over the lower part of the Chiufen Chi.

4. GEOPHYSICAL PROSPECTING

From August, 1989 to May, 1990, Transient Electro-Magnetic (TEM) soundings were conducted in the study area. The purpose of this TEM survey was to map the groundwater flow system and related basement topography. A total of 49 coincident-loop TEM soundings (Figure 5) were made with 20 meters as a loop side length. The relatively small dimensions of the transmitter array, with an effective exploration depth of between 5 m to 50 m, allowed TEM surveys to be the only proper geophysical method to operate in this hilly area with limited open spaces.

The basic principle of the TEM method of geophysical prospecting is shown in Figure 6. The driving current flowing in a transmitter loop sets up a magnetic field and induces eddy currents to flow in any good electrical conductor in the ground as it is switched off. These eddy currents set up a secondary magnetic field which can be detected by a receiver loop as a time-dependent decaying voltage. The recording of the "transients" is a means of detecting conductors in the ground. The decaying transient can be described by a number of measurement channels recording the voltage at various delay times during the "quiet time" between current pulses. The character of this decay (duration, amplitude, etc.) depends on the conductivity, shape and size, depth and attitude of the conductor and its position with respect to the receiver loop.

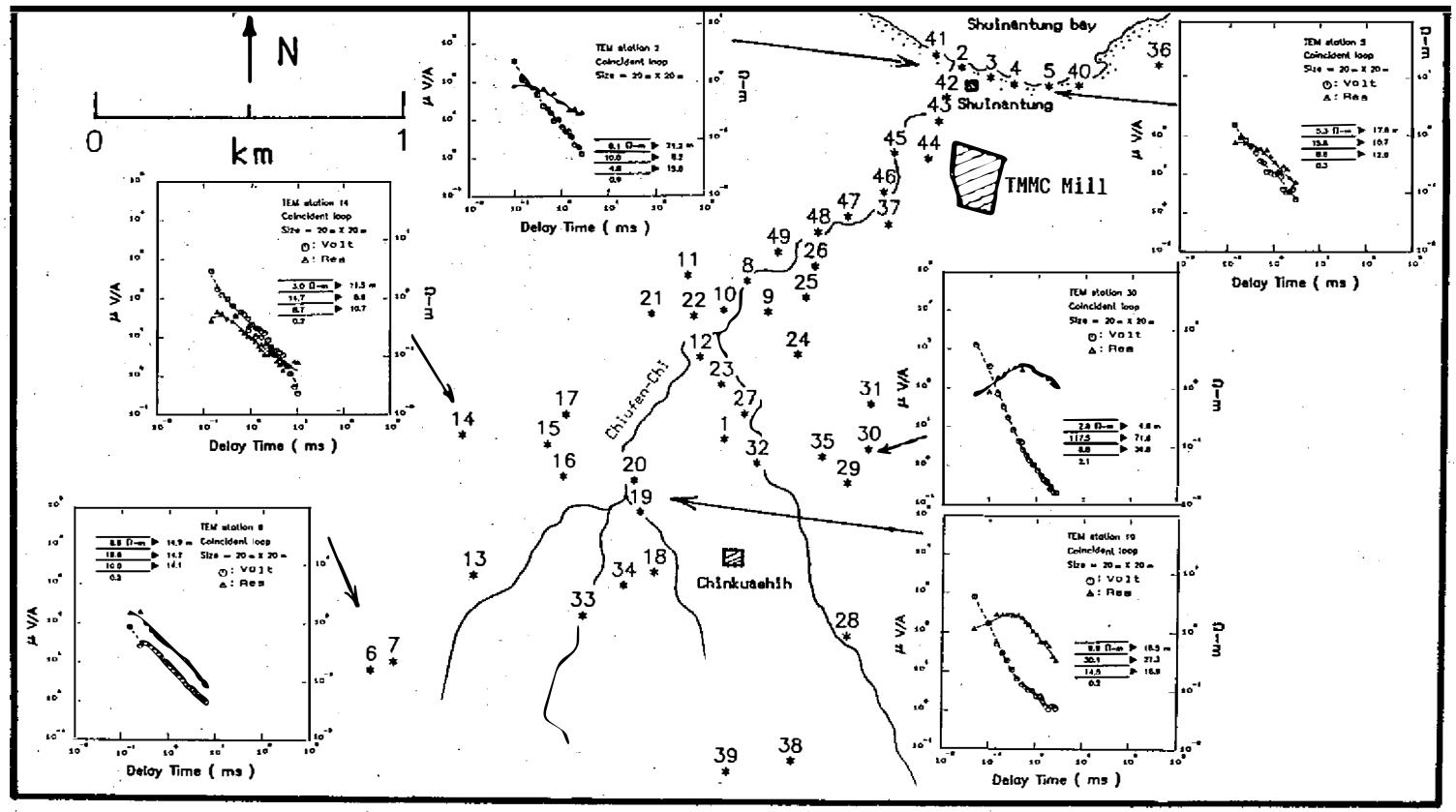

Fig. 5 Locations of the TEM sounding points, with some typical invered results showing in the Chinkuashih-Shuinantung area.

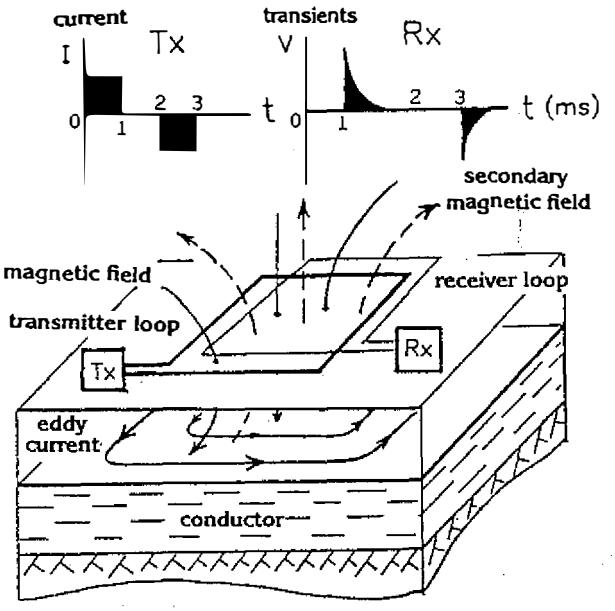

Fig. 6 Principle of the coincident loop TEM sounding.

It can also be used to provide information on all of these factors (Knight and Raiche, 1982; Raiche, *et al.*, 1985; Raiche and Spies, 1981). Furthermore, the receiver-transmitter array of the TEM does not need to be widened in order to obtain deeper subsurface information. The depth of investigation for the TEM method is mainly a function of the recorded transient time.

SIROTEM II SE (CSIRO, Australia) was used in this TEM survey. Each measurement was recorded by stacking up to 512 readings before they were printed out. These SIROTEM data were then inverted, with the aid of the Jupp-Vozoff inversion scheme (1975), to give the thickness and resistivities of the stratigraphic layers for quantitative interpretation. Four-layered models consisting of low-high-low-low resistivity patterns best fit the field data. Some of the typical field data and their inverted results were also shown in Figure 5. Consequently, without having other geophysical or geologic information strongly suggesting the use of models having more layers, we used a four-layer model for interpretations.

The inverted TEM results at different depths were contoured and shown as a depth slice map in Figure 7. In the two extremities of this area, i.e. SW and NE parts, resistivities were low, while high resistivities (more than 200 $ohm-m$) predominated in between. The lower resistivities were interpreted as an overburden with a saturated aquifer while the higher resistivities indicate basement rock. From Figure 7, it is clear that the saturated aquifer was interrupted by the basement rock in the central part of the area. Moreover, the SW-NE trend

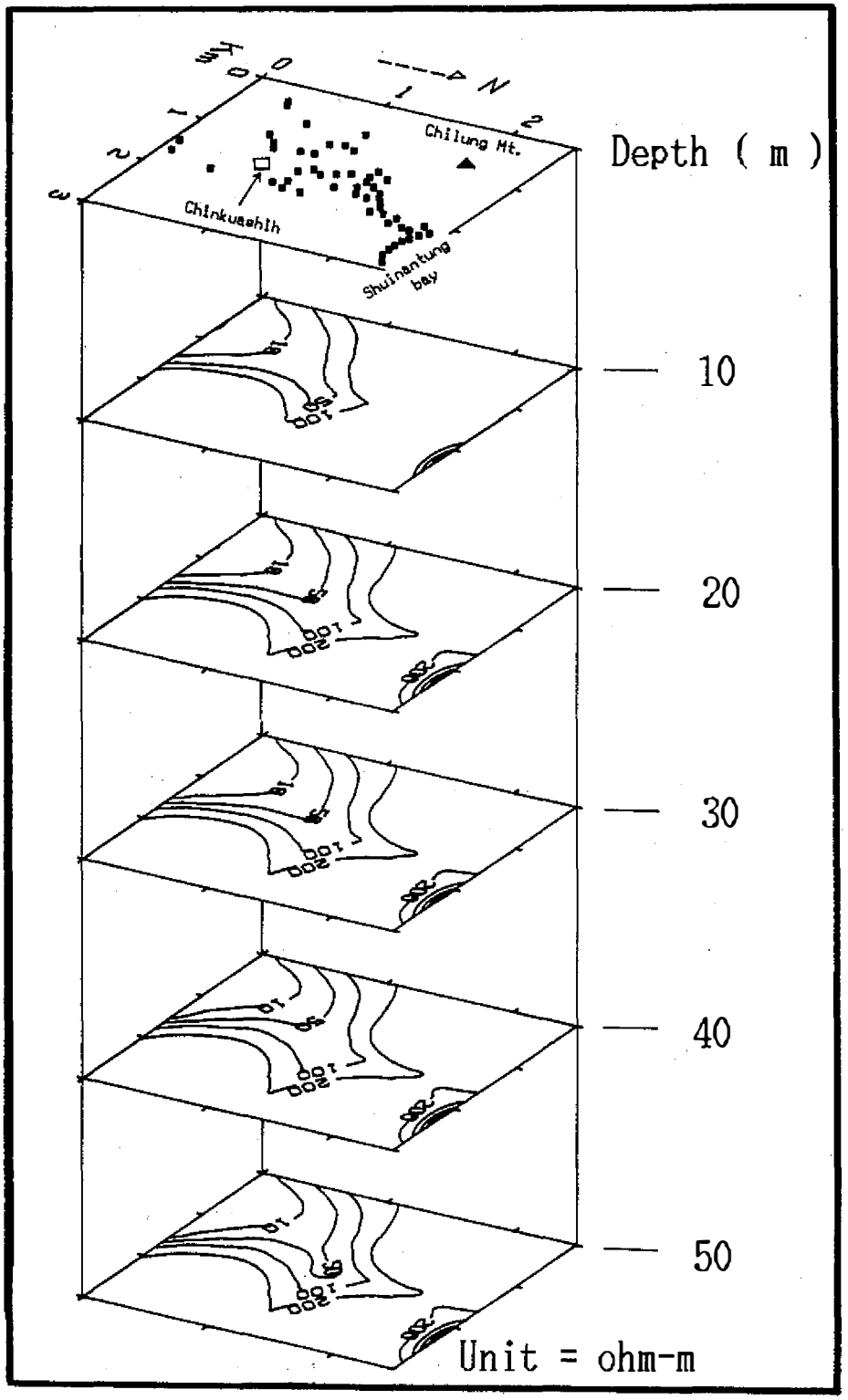

Fig. 7 Depth slice of resistivity in the Chinkuashinh-Shuinantung area.

of the saturated aquifer is close to the course of the Chiufen Chi, indicating a close relationship between surface water flow pattern and the groundwater flow system. Therefore, the location and dimensions of those low resistivities in the depth slice map can be used to estimate the direction and extent of groundwater migration in 3-D space for this area.

For the purposes of clarity, an additional 3-D plot of surface and basement topography is drawn in Figure 8, inferred from the thickness of resistivities less

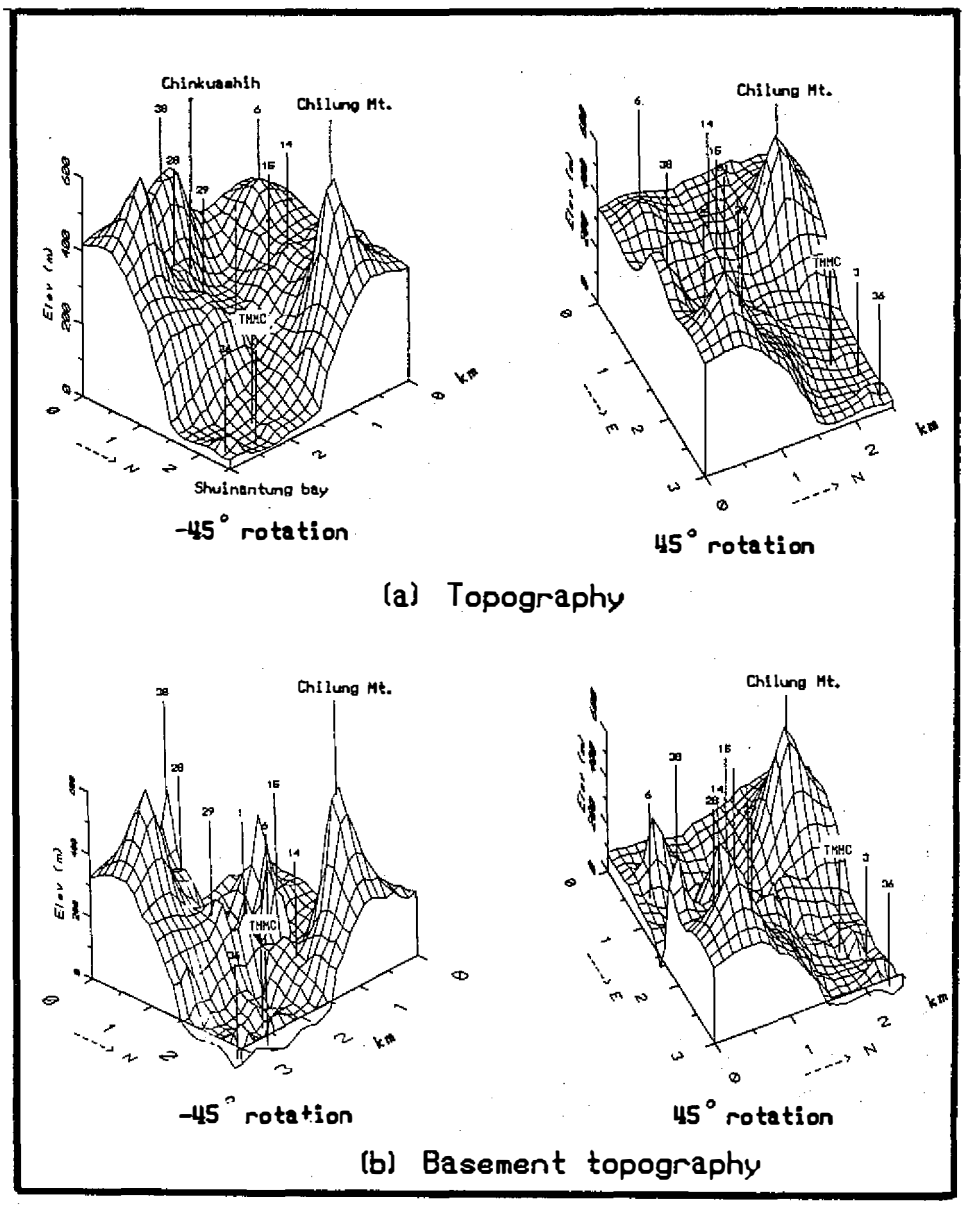

Fig. 8 Three-dimensional plots of the Chinkuashih-Shuinantung area ; (a) Topography, (b) Basement topography.

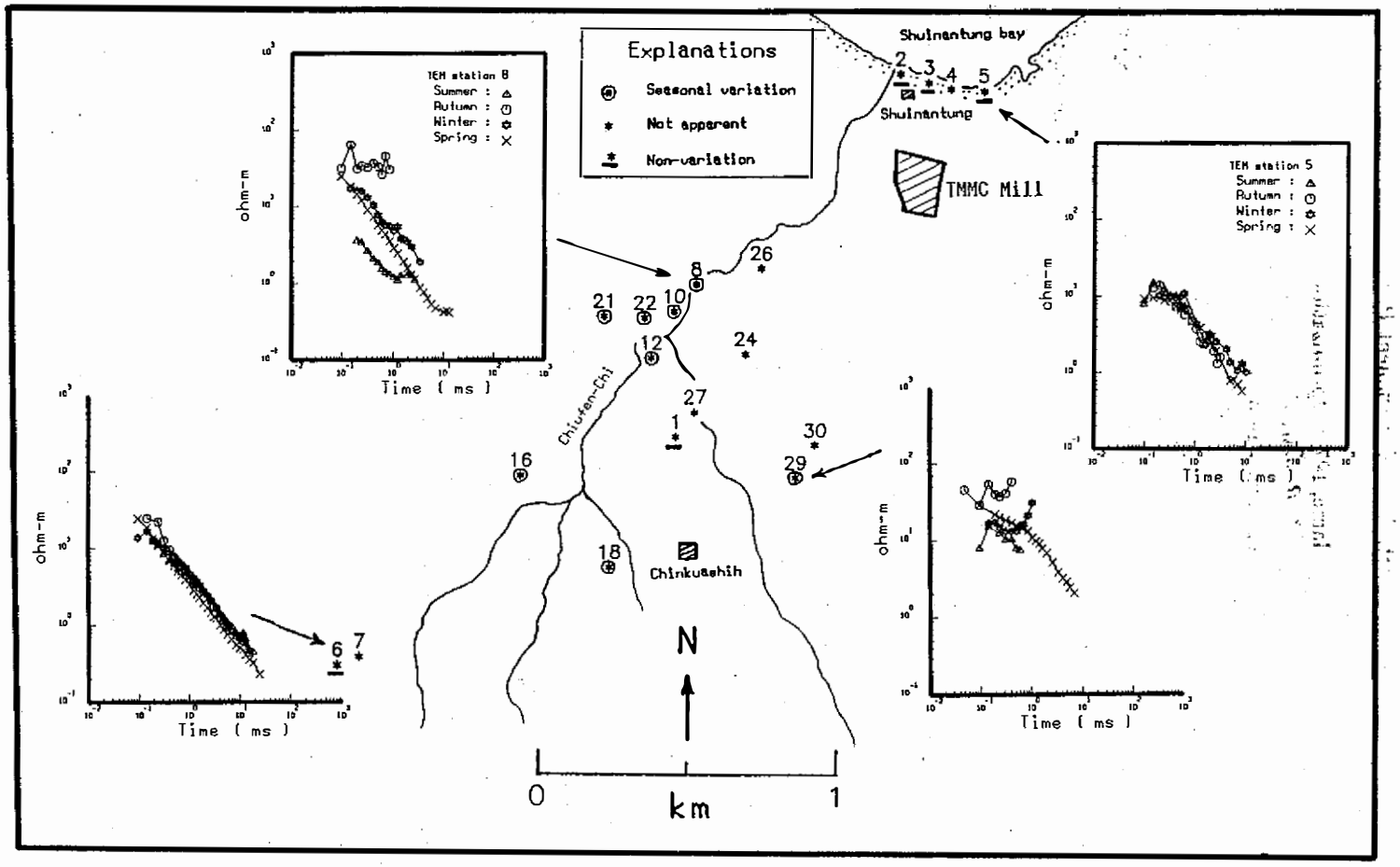

Fig. 9 Sites of seasonal variation of resistivities, with some typical data shown in the Chinkuashih-Shuinantung area.

than 20 $ohm - m$ as overburden. These maps had been rotated 45 and -45 degrees respectively. The groundwater flowing from SW to NE is rather clear: It is roughly parallel to the surface water system.

In order to check whether resistivity varied with season in the study area, some of the TEM data (Figure 9) were collected and analyzed during each season of a year. The results indicate that resistivities from the Chiufen Chi varied with the season, indicating high porosity and permeability under the study area. On the other hand, resistivities measured along the Shuinantung Bay were not affected by seasonal changes, indicating a saturated aquifer underneath the area near the the sea.

In summary, the TEM results are listed as follows:

(1) The groundwater flow is from southwest to northeast roughly parallel to the surface water system.

(2) Water table configurations of the area study are a gentle reflection of the topography, and also generally changed with the season.

(3) Using square loops 20 m on a side, four layers were mapped to a depth greater than 50 m. This demonstrates the effectiveness of the TEM technique for delineating both groundwater flow and basement topography, especially in hilly areas.

5. CONCLUSIONS

(1) Surface water and soil were high in iron, copper and sulfate contents, especially throughout the lower stream area of the Chiufen Chi.

(2) Resistivities measured along the Chiufen Chi varied with the season, indicating high porosity and permeability under the study area, probably due to ore mineralization and/or crustal movements. Good passages for ground water can be expected throughout the area.

(3) Resistivities measured along the Shuinantung Bay were not affected by seasonal change, indicating a saturated aquifer underneath the area near the sea.

(4) Acid mine drainage from the Chinkuashih is concluded to be the main reason to cause marine and river pollution over the Shuinantung area.

Acknowledgements. The authors would like to extend their gratitude to Dr.Kung-Tu Kuo and his research assistants,for performing all of the chemical analyses.Gratitude is further extended to two anonymous reviewers of this manuscript for giving helpful comments and suggestions. This research project was financially supported by a grant from the Taiwan Power Company.

REFERENCES

Chen, C. C. 1986: Copper and gold mineralization in the Chinkuashih area, northern Taiwan; *Proc. Geol. Soc. China*, **29**, pp 63–71.

Huang, C. K. 1955: Gold-copper deposits of the Chinkuashih mine, Taiwan, with special reference to the mineralogy; Acta Geologica Taiwanica, *Sci Rept of the National Taiwan University.*, **7**, pp 1–20.

——, 1963: Factors controlling the gold-copper deposits of the Chinkuashih mine, Taiwan; Acta Geologica Taiwanica, *Sci Rept of the National Taiwan University.*, **10**, pp 1–9.

Huang, C. K. and Yeh, K. S. 1977: Special features of the Changjen Series, Chinkuashih mine, Taiwan; Acta Geologica Taiwanica, *Sci Rept of the National Taiwan University.*, **19**, pp 1–12.

Juan, V. C., Wang, Y. and Sun, S. S. 1959: Hydrothermal alteration of dacite at the Chinkuashih mine, Taipeihsien, Taiwan; *Proc. Geol. Soc. China*, **2**, pp 73–92.

Jupp, D. L. B. and Vozoff, K. 1975: Stable iterative method for geophysical inversion; *Geophys. J. Roy. Soc.*, **42**, pp 957–976.

Knight, J. and Raice, A. P. 1982: Transient electromagnetic calculations using the Gaver-Stehfest inverse Laplace transform method; *Geophysics*, **47**, pp 47–50.

Raiche, A. P., Jupp, D. L. B., Rutter, H., Vozoff, K. 1985: The joint use of coincident loop transient electromagnetic and Schlumberger sounding to resolve layered structures; *Geophysics*, **50**, pp 1618–1627.

Raiche, A. P., Spies, B. R. 1981: Coincident loop transient electromagnetic master curves for interpretation of two-layer earth; *Geophysics*, **46**, pp 53–64.

Tan, L. P. and Yu, F. S. 1968: Heavy-mineral reconnaissance for gold and copper deposits of the Chinkuashih mine, Taiwan; Acta Geologica Taiwanica, *Sci Rept of the National Taiwan University*, **12**, pp 41–57.

Wang Y. 1953: Geology of the Chinkuashih and Chiufen districts, Taipeihsien, Taiwan; Acta Geologica Taiwanica, *Sci Rept of the National Taiwan University*, **5**, pp 47–64.

——, 1955: Fracture patterns in Chinkuashih area, Taipeihsien, Taiwan; Acta Geologica Taiwanica, *Sci Rept of the National Taiwan University*, **7**, pp 21–33.

——, 1973: Wall rock alteration of late Cenozoic mineral deposits in Taiwan; geologic settings and field relations; *Proc. Geol. Soc. China*, **16**, pp 145–160.

Yen, T. P. 1974: Structural controls of the metallic deposits in Taiwan; *Proc. Geol. Soc. China*, **17**, pp 111–122.

Appendix: The results of geochemical analyses.

		T1	T2	T3	T4	T5	T6	T7	T8	T9	T10	T11	AV.	SD.
pH	S	4.91	5.13	2.57	2.70	5.61	4.80	4.73	5.95	2.54	3.25	2.58	4.07	1.28
	M	6.72	6.82	4.97	6.56	6.90	6.09	4.40	6.58	2.43	3.00	2.45	5.17	1.74
	F	7.1	7.5	4.9	6.8	5.2	6.0	4.5	7.3	2.2	3.1	2.3	5.17	1.88
	W	6.7	6.9	2.6	6.0	6.6	6.1	6.3	6.3	2.4	3.1	2.5	5.05	1.83
	AV	6.36	6.59	3.76	5.51	6.08	5.75	4.98	6.53	2.39	3.11	2.46	Unit : ppm	
	SD	0.85	0.88	1.18	1.65	0.70	0.55	0.77	0.50	0.12	0.09	0.10		
TS	S	180	100	1950	1710	210	70	200	40	4780	620	4470	1302.73	1689.68
	M	250	120	200	620	100	90	170	150	900	390	1530	410.91	428.16
	F	160	660	320	730	240	180	150	290	3350	660	3090	893.64	1116.60
	W	190	195	7090	870	155	120	85	175	11650	1940	11935	3127.73	4527.66
	AV	165.00	268.75	2390.00	982.50	176.25	115.00	151.25	163.75	5170.00	902.50	5256.25	Unit : ppm	
	SD	33.54	228.65	2800.21	429.27	53.55	41.53	42.19	88.84	3990.23	607.80	3993.79		
SS	S	30	10	70	110	30	10	30	10	100	120	250	70.00	69.41
	M	60	40	40	70	70	70	50	80	70	100	50	63.64	17.20
	F	80	60	110	60	130	140	140	260	50	140	60	111.82	58.44
	W	15	35	15	15	25	45	10	20	40	20	20	23.64	10.89
	AV	46.25	36.25	58.75	63.75	63.75	66.25	57.50	92.50	65.00	95.00	95.00	Unit : ppm	
	SD	25.34	17.81	35.42	33.80	42.04	47.61	49.69	100.34	22.91	45.55	90.69		
COND	S	156.0	227	2470	2139	170	84	177	194	4030	727	3980	1304.91	1499.58
	M	612	310	394	931	214	118	249	290	3060	760	3100	912.55	1048.35
	F	201	226	366	874	249	116	249	290	3060	760	3110	862.82	1069.11
	W	146	143	2250	885	167	85	167	177	5710	877	5990	1508.82	2136.12
	AV	278.75	226.50	1370.00	1207.25	200.00	100.75	210.50	237.75	3965.00	781.00	4042.50	Unit : ppm	
	SD	193.51	59.04	993.10	538.37	33.86	16.27	38.66	52.59	1082.51	57.04	1180.39		
DO	S	1.8	2.0	1.6	2.8	1.9	1.8	1.7	1.5	1.1	1.9	0.9	1.73	0.47
	M													
	F	0.2	0.1	0.1	0.2	0.6	0.1	0.1	0.3	0.1	0.1	0.1	0.18	0.15
	W	0.1	0.1	0.2	0.1	0.1	0.2	0.2	0.1	0.1	0.2	0.1	0.15	0.07
	AV												Unit : μ S/cm	
	SD													
COD	S	1.5	1.1	1.8	1.6	1.3	1.1	0.6	2.4	2.8	1.2	8.4	2.16	2.06
	M	37.0	36.0	37.0	34.5	25.5	26.5	25.5	16.0	15.0	15.5	16.0	25.86	8.77
	F	9.5	5.0	10.0	12.5	19.0	12.0	7.0	13.5	50.0	17.0	39.0	17.68	13.41
	W	5.0	4.5	17.0	4.0	4.0	7.0	3.5	3.0	19.5	14.5	18.0	9.09	6.34
	AV	13.25	11.65	16.45	13.15	12.45	11.65	9.15	8.73	21.83	12.05	20.35	Unit : ppm	
	SD	14.00	14.14	13.03	12.97	10.11	9.40	9.71	6.09	17.38	6.33	11.35		
S=	S	0.018	---	---	0.009	---	---	---	0.001	0.002	---	0.004	0.00	0.01
	M	0.058	0.008	0.057	---	0.055	0.014	0.022	0.004	0.077	0.002	0.043	0.03	0.03
	F	---	0.833	10478	---	---	1.239	---	0.818	0.724	1.775	1.760	0.78	0.68
	W	0.005	0.101	0.112	0.035	0.038	0.097	0.033	0.088	0.117	0.098	0.123	0.08	0.04
	AV	0.02	0.24	0.41	0.01	0.02	0.34	0.01	0.23	0.23	0.47	0.48	Unit : ppm	
	SD	0.02	0.35	0.62	0.02	0.02	0.52	0.01	0.34	0.29	0.76	0.74		

		T1	T2	T3	T4	T5	T6	T7	T8	T9	T10	T11	AV.	SD.
SO_4	S	15.2	14.8	110.3	94.6	21.4	3.3	2.05	1.23	91.35	57.60	106.16	47.09	43.25
	M	65.85	86.43	234.60	448.62	90.54	78.20	86.43	45.27	1395.25	209.90	1588.69	393.62	531.07
	F	114.4	241.1	253.3	412.6	379.9	408.5	612.76	604.59	1454.29	269.61	1723.91	588.63	495.98
	W	20	10	2910	950	120	70	170	270	3540	680	3080	1074.55	1323.61
	AV	53.86	88.08	877.05	476.45	152.96	140.00	217.81	230.27	1620.22	304.28	1624.69	Unit : ppm	
	SD	40.16	93.39	1175.01	306.15	135.82	157.72	235.63	238.94	1235.02	230.29	1052.97		
Fe	S	---	---	196	140	---	---	---	---	730	2.86	894	178.44	307.47
	M	0.21	0.17	0.30	0.15	0.16	0.18	0.21	0.19	41.90	4.19	41.70	8.12	15.92
	F	---	---	---	---	---	---	---	---	309.5	5.63	301.5	56.06	117.61
	W	2.19	2.20	3600	2.61	2.54	2.50	2.43	2.44	2040	39.7	2204	718.24	1217.54
	AV	0.60	0.59	949.08	35.69	0.68	0.67	0.66	0.66	780.35	13.10	860.30	Unit : ppm	
	SD	0.92	0.93	1532.60	60.23	1.08	1.06	1.03	1.03	767.51	15.39	835.02		
Cu	S	0.68	0.35	24.3	34.5	0.44	0.25	0.89	0.25	55.7	4.73	54.1	16.02	21.35
	M	---	---	1.41	3.85	0.05	0.10	0.58	---	7.37	3.61	7.37	2.21	2.78
	F	---	---	1.03	---	---	---	0.75	---	46.5	5.73	30.5	7.68	15.01
	W	0.02	0.11	37.0	22.9	1.37	0.05	1.06	0.01	23.7	9.27	29.0	11.32	13.40
	AV	0.17	0.11	15.63	15.31	0.47	0.10	0.82	0.06	33.32	5.84	30.24	Unit : ppm	
	SD	0.29	0.14	15.39	14.07	0.55	0.09	0.18	0.11	18.98	2.12	16.54		
Zn	S	---	---	2.09	2.95	---	---	---	---	11.35	---	12.15	2.59	4.43
	M	0.027	0.041	0.386	1.519	0.063	0.072	0.125	0.058	2.366	0.338	2.735	0.70	0.97
	F	0.139	0.155	0.710	2.419	0.376	0.211	0.326	0.188	2.344	0.618	3.274	0.98	1.08
	W	0.03	0.09	2.62	3.45	0.15	1.06	0.03	0.05	20.18	0.52	18.94	4.28	7.29
	AV	0.05	0.07	1.45	2.58	0.15	0.34	0.12	0.07	9.06	0.37	9.27	Unit : ppm	
	SD	0.05	0.06	0.93	0.72	0.14	0.42	0.13	0.07	7.40	0.24	6.72		
Mn	S	0.04	0.05	3.53	2.57	---	---	0.05	6.22	7.19	6.53	4.74	2.81	2.82
	M	0.17	0.07	0.73	0.54	0.14	0.05	0.35	0.15	4.74	1.50	4.63	1.19	1.70
	F	0.13	0.08	0.80	0.60	0.17	---	0.25	---	2.88	1.19	3.93	0.91	1.25
	W	---	0.12	4.57	2.89	---	0.13	---	---	8.86	0.86	9.66	2.46	3.50
	AV	0.09	0.08	2.41	1.65	0.08	0.04	0.16	1.59	5.92	2.52	5.74	Unit : ppm	
	SD	0.07	0.03	1.68	1.09	0.08	0.05	0.14	2.67	2.29	2.33	2.28		
Pb	S	---	---	---	---	---	---	---	---	---	---	---	---	---
	M	0.05	0.02	---	0.04	0.04	0.08	0.06	0.06	0.07	0.08	0.08	0.05	0.02
	F	---	---	---	---	---	---	---	---	---	---	---	---	---
	W	0.32	0.55	0.18	---	---	---	---	0.38	---	---	---	0.13	0.19
	AV	0.09	0.14	0.05	0.01	0.01	0.02	0.01	0.11	0.02	0.02	0.02	Unit : ppm	
	SD	0.13	0.24	0.08	0.02	0.02	0.03	0.03	0.16	0.03	0.03	0.03		
Ca + Mg	S	19.63	34.74	566.5	1472.8	43.80	12.08	46.82	31.72	3474.3	528.7	4342.9	961.27	1462.98
	M	111.93	99.99	315.94	507.24	73.13	30.15	92.53	75.36	*	831.89	*		
	F	58.82	75.53	207.35	211.76	35.29	22.06	91.18	63.24	3750.00	110.29	3088.24	701.07	1290.39
	W	30.0	45.71	2535.7	225.7	45.71	35.71	87.14	40.0	3392.8	735.7	3964.2	1012.58	1445.53
	AV	55.10	63.49	906.37	604.38	49.48	25.00	79.42	52.58		551.65		Unit : ppm	
	SD	35.82	25.38	949.67	515.06	14.21	8.90	18.92	17.51		277.37			

		R1W	R2W	R3W	R4W	R5W	R6W	R7W	R8W	AV.	SD.
pH	S	4.62	6.45	6.35	6.56	6.29	6.83	5.45	3.00	5.69	1.22
	M	6.7	6.6	5.4	7.5	5.2	4.8	6.7	3.5	5.80	1.22
	F	2.48	6.00	5.47	4.09	4.54	4.06	5.32	3.40	4.42	1.09
	W	3.90	6.46	6.91	7.49	6.87	6.81	7.15	3.07	6.08	1.54
	AV	4.43	6.38	6.03	6.41	5.72	5.63	6.15	3.24	Unit : ppm	
	SD	1.52	0.23	0.63	1.39	0.91	1.22	0.79	0.21		

Fe	S	0.09	—	—	0.04	—	—	0.14	13.48	1.72	4.45
	M	0.52	—	3.41	5.24	0.29	—	2.07	10.31	2.73	3.36
	F	7.75	5.34	5.57	5.59	5.59	5.69	6.01	6.04	5.95	0.72
	W	2.46	2.40	2.82	2.36	2.46	2.34	5.00	1386	175.73	457.44
	AV	2.70	1.94	2.95	3.31	2.09	2.01	3.31	353.96	Unit : ppm	
	SD	3.05	2.20	1.99	2.26	2.24	2.33	2.33	595.86		

Cu	S	0.27	0.25	0.27	0.69	0.31	0.29	0.36	7.27	1.21	2.29
	M	0.13	0.02	0.13	0.18	0.02	0.23	0.34	5.17	0.78	1.66
	F	0.24	—	0.01	0.06	—	0.02	0.03	1.30	0.21	0.42
	W	—	0.01	0.56	0.03	—	0.01	0.57	4.95	0.77	1.60
	AV	0.16	0.07	0.24	0.24	0.08	0.14	0.32	4.67	Unit : ppm	
	SD	0.11	0.10	0.21	0.21	0.13	0.12	0.19	2.15		

Zn	S	—	—	—	—	—	—	—	0.67	0.08	0.22
	M	0.05	—	0.06	0.11	0.06	0.35	0.02	0.53	0.15	0.18
	F	0.39	0.07	0.58	0.19	0.10	0.26	0.16	0.56	0.29	0.19
	W	0.15	0.08	0.03	—	—	—	0.06	0.59	0.11	0.19
	AV	0.15	0.04	0.17	0.08	0.04	0.15	0.06	0.59	Unit : ppm	
	SD	0.15	0.04	0.24	0.08	0.04	0.16	0.06	0.05		

Mn	S	—	—	0.17	0.05	—	—	—	0.80	0.13	0.26
	M	0.03	0.01	0.05	0.16	0.08	0.99	0.04	0.69	0.26	0.35
	F	6.23	0.19	0.02	0.25	0.02	0.39	0.02	0.89	1.00	1.99
	W	0.96	0.59	—	—	—	0.06	0.03	0.64	0.28	0.36
	AV	1.80	0.20	0.06	0.12	0.02	0.36	0.02	0.75	Unit : ppm	
	SD	2.58	0.24	0.07	0.10	0.03	0.39	0.01	0.10		

Pb	S	—	—	—	—	—	—	—	—	0.00	0.00
	M	0.09	0.09	0.11	0.12	0.12	0.13	0.13	0.14	0.10	0.04
	F	—	—	—	0.02	—	—	—	—	0.00	0.01
	W	—	—	—	—	—	—	—	—	0.00	0.00
	AV	0.02	0.02	0.03	0.04	0.03	0.03	0.03	0.04	Unit : ppm	
	SD	0.04	0.04	0.05	0.05	0.05	0.06	0.06	0.06		

		R1A	R2A	R3A	R4A	R5A	R6A	R7A	R8A	AV.	SD.
Fe	S	3100	40800	1580	2750	2820	1550	3070	1340	7126.25	12745.67
	M	26.64	26.19	26.13	26.41	26.41	26.61	26.67	26.66	26.47	0.20
	F	1100	8388	546	608	644	978	1200	1446	1863.75	2483.70
	W	3404	12680	1676	2448	2084	2312	3672	2772	3881.00	3382.49
	AV	1907.66	15473.55	957.03	1458.10	1393.60	1216.65	1992.17	1396.17	Unit : ppm	
	SD	1401.00	15313.87	696.51	1164.19	1111.57	834.28	1455.53	971.35		
Cu	S	8.60	571	101	136	90	107	153	118	160.57	160.24
	M	4.57	9.26	10.45	10.52	7.43	9.55	10.47	10.60	9.11	1.98
	F	5.67	14.98	30.60	26.90	6.70	14.30	98.60	21.70	27.43	28.15
	W	9.61	37.0	68.0	9.81	49.0	250	67.0	0.61	61.38	75.36
	AV	7.11	158.06	52.51	45.81	38.28	95.21	82.27	37.73	Unit : ppm	
	SD	2.06	238.64	34.79	52.52	34.42	97.45	51.62	46.94		
Zn	S	21	503	2.77	29	47	32	36	23	87.72	157.79
	M	5.81	5.85	5.34	6.01	5.90	6.36	6.52	5.54	5.92	0.36
	F	15.0	193.0	17.5	17.0	22.5	25.5	21.0	27.0	42.31	57.09
	W	5.94	125.0	50.0	23.0	23.0	24.0	29.0	2.79	35.34	36.49
	AV	11.49	206.71	18.90	18.75	24.60	21.97	23.13	14.58	Unit : ppm	
	SD	6.42	183.71	18.80	8.49	14.65	9.50	10.96	10.56		
Mn	S	29	9.93	11.40	52	162	40	108	427	104.92	131.13
	M	8.66	8.60	6.07	8.70	8.72	8.70	8.71	0.91	7.38	2.59
	F	56.5	46.0	26.0	43.5	80.0	76.0	34.0	29.0	48.88	19.17
	W	33.0	29.0	134	90.0	160	46.0	67.0	67.0	78.25	44.29
	AV	31.79	23.38	44.37	48.55	102.68	42.67	54.43	130.98	Unit : ppm	
	SD	16.99	15.35	52.26	28.91	63.54	23.89	37.20	172.51		
Pb	S	8.23	7.29	1.78	4.32	3.63	4.67	11.27	7.95	6.14	2.87
	M	0.88	1.91	1.76	4.26	2.38	6.13	9.78	3.47	3.82	2.73
	F	1.25	6.25	2.74	2.07	2.07	3.49	3.92	1.23	2.88	1.56
	W	3.75	11.54	4.01	8.11	4.80	5.80	18.14	12.30	8.56	4.75
	AV	3.53	6.75	2.57	4.69	3.22	5.02	10.78	6.24	Unit : ppm	
	SD	2.93	3.42	0.92	2.17	1.08	1.04	5.06	4.26		

T1–T11 : water sample;
R1W–R8W : water-washed soil sample;
R1A–R8A : nitric acid-washed soil sample;
TS : total sediment, in ppm;
SS : suspensed sediment, in ppm;
Cond : conductivity, in μS/cm;
DO : dissolved oxygen, in ppm;
COD : chemical oxygen demand, in ppm;

S : Spring;
M : Summer;
F : Fall;
W : Winter;
AV : average;
SD : standard deviation;
--- : trace to not determinable;
* : titration failed due to high Fe content.

金瓜石－水湳洞地區之酸性礦山排水

蔡龍珆、陳洲生、孫立中
中央大學地球物理研究所

摘要

金瓜石－水湳洞地區地表地層以中新世南港層爲主，自晚上新世起之地殼運動造成多條高角度斷層，並將石底層抬升至地表出露，進而導致更新世石英安山岩之侵入與熱水換質形成之金、銅礦體；礦床分佈以測區南側之本山礦體爲主，多爲硫化金屬礦，爲造成酸礦排水之典型礦體。測區主要河川爲九份溪主、支流，逕流大抵與斷層線相近，顯示受斷層作用形成破碎帶後匯流成河。

測區經實地勘察後，擇定於金瓜石本山五坑坑口、七坑坑口、水湳洞南側海邊近本山七坑坑口排水孔處、水湳洞東側及西側、九份溪主流（上游、中游、下游）與九份溪支流採取地表水樣及土樣。分別進行pH值、水溫、濁度、電導度、溶氧量和多項離子濃度之地化分析。結果指出本山五坑、七坑二排水口處酸性強、金屬含量高、電導度強，表現酸性礦山排水效應。

以20公尺方型共圈之暫態電磁波法測勘，共計49點，各測點資料施以一維逆推，可以四層低－高－低－低電阻之電性地層模型擬合之，有效探查深度約爲5公尺至50公尺。各層地電阻分佈顯示電性地層不連續面與斷層構造有關，且爲地下水良好通路，地下水流向則大抵均匯流後朝東北方向移動出海。